EFFECT OF SECOND-PHASE DOPING ON LASER DEPOSITED Al_2O_3 CERAMICS

F.Y. Niu[1], D.J. Wu[1], G.Y. Ma[1], S.Y. Zhou[1], B. Zhang[1,2]*

1. Key Laboratory for Precision and Non-Traditional Machining Technology of Ministry of Education, Dalian University of Technology, Dalian, Liaoning, China, 116024
2. Department of Mechanical Engineering, University of Connecticut, Storrs, CT 06269, USA

REVIEWED

Abstract

Direct fabrication of engineering ceramic components by additive manufacturing (AM) is a relatively new method for producing complex mechanical structures. This study investigates how a second-phase doping may affect Al_2O_3 ceramic parts deposited by AM with a laser engineered net shaping (LENS) system. In this study, ZrO_2 and Y_2O_3 powders are respectively doped into Al_2O_3 powders at the eutectic ratio as second-phases to improve the quality of a deposited part. The deposited Al_2O_3, Al_2O_3/ZrO_2 and Al_2O_3/YAG (yttrium aluminum garnet) parts are examined for their micro-structures and micro-hardness, as well as defects. The results show that doping of ZrO_2 or Y_2O_3 as a second-phase performs a significant role in suppressing cracks and in refining grains of the laser deposited parts. The micro-hardness investigation reveals that the second-phase doping does not result in much hardness reduction in Al_2O_3 and the two eutectic ceramics are both harder than 1500 Hv. The study concludes that the second-phase doping is good for improving laser deposited ceramic parts.

1. Introduction

Engineering ceramics is an irreplaceable material used in the extreme working conditions due to their excellent mechanical properties, as well as thermal and chemical resistances [1]. However, traditional manufacturing methods for engineering ceramic parts have difficulties in meeting the requirements from the fast-developing modern technology because of their limitations, such as low sintering efficiency, limited complexity of fabricated structures and relatively low strength [2, 3]. The limitations mostly arise from batching, forming, sintering and machining, which are the main processing steps in the traditional manufacturing methods. Therefore, it is significant to develop new processing methods for making full use of engineering ceramics.

Ceramic additive manufacturing is a newly developed method in recent decades and has been successfully demonstrated for its advantages with the use of “indirect” and “direct” methods. By the indirect method, a green body is first created from ceramic powders or slurry with a high content of an organic or inorganic binder, and then sintered and densified to eliminate binders. Because a high energy source is not needed, many indirect processing methods have been

developed, such as stereo lithography (SL), laminated object manufacturing (LOM), fused deposition of ceramics (FDC) and freeze-form extrusion fabrication (FEF), etc. [4-8]. Through these methods, complex geometries can be obtained, but limitations, such as impurities, porosities and shrinkage, still exist because the processing steps are the same as in the traditional methods. On the other hand, with the direct method, pure ceramic powders can be melted directly by a high energy source and then the melt pool solidifies to form a part. Due to the melting/solidification processes, fully densified ceramic parts with good performances are produced more easily and rapidly. Comparatively, few direct processing methods, e.g., laser engineered net shaping (LENS) and selective laser melting (SLM), have been developed because of the need for a high energy source [9-14]. Wilkes et al. manufactured ceramic parts from ZrO_2/Al_2O_3 powders with an SLM system and obtained crack-free specimens with flexural strength higher than 500 MPa [9, 10]. Balla et al. used an LENS system to fabricate dense and net-shaped structures of Al_2O_3 and obtained cylindrical, cubic and gear-shaped parts which showed microstructural anisotropy with hardness of 1550 Hv [11, 12]. Bertrand et al. applied SLS/M to manufacturing net shaped parts from the pure yttria-zirconia powders and demonstrated possibility of processing pure ceramic powders by SLM without doping [13,14].

Although the direct methods have demonstrated many advantages in fabricating ceramic parts, there are also technical challenges, such as crack control and property improvements in the laser-aided processes due to the hard and brittle properties of a ceramic material as well as large thermal gradients generated during laser radiation. Preheating was proposed by Wilkes and has been proven to be an effective method for suppressing cracks generated by the SLM fabrication [10]. However, this method provided a limited preheating area and poor surface quality. Because the direct additive manufacturing methods of ceramic parts have been developed in a relatively short time, they need to be further developed for industrial applications.

In this study, an LENS system is used to fabricate ceramic single-bead walls directly from ceramic powders. A new method of second-phase doping is proposed to improve quality of a deposited part. ZrO_2 and Y_2O_3 powders are respectively doped into Al_2O_3 powders at their respective eutectic ratios as a second-phase to verify the proposed method. Micro-structure and micro-hardness of the fabricated parts are then investigated.

2. Experimental procedures

The LENS experimental system used in this study is shown in Figure 1. The system consisted of a 1000 W Nd:YAG laser, an automatic powder feeder with three containers, and a numerically controlled worktable. A Ti-6Al-4V plate of 6 mm thick was used as a substrate for ceramic deposition due to its high laser absorptivity and good compatibility with the ceramics. For an efficient use of the ceramic powders, the focus of the powder stream was set on the surface of the substrate. Pure argon was used as a protective gas for separating the fabricated part from the atmosphere.

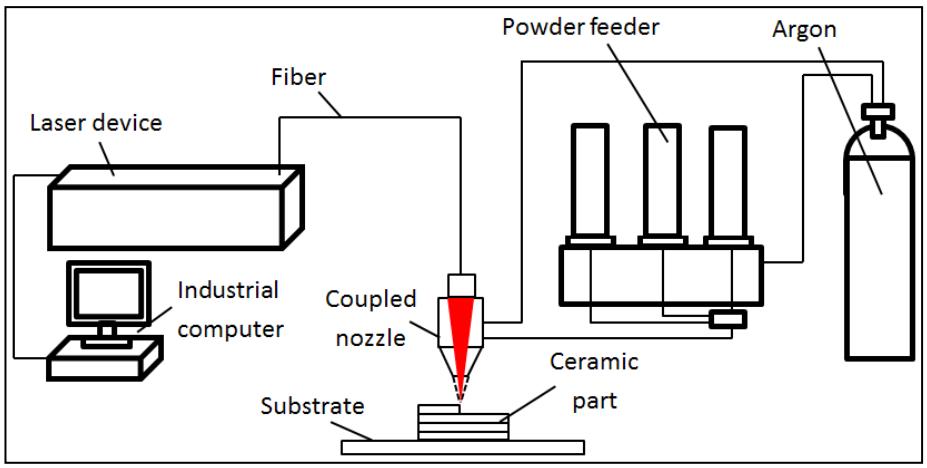

Figure 1 Experimental system of LENS

Al_2O_3, ZrO_2 and Y_2O_3 ceramic powders (purity wt%>99.5%) of particle sizes in the range of 42-90 μm were used for all the experiments after drying at 100 ℃ for 4 hours to eliminate moisture. The three ceramic powders were loaded into the respective containers of a powder feeder. Flow rate of the powders was independently controlled. In this study, fabrication of Al_2O_3/ZrO_2 parts was conducted by mixing ceramic powders at the eutectic ratio of 58.5 wt% Al_2O_3 and 41.5 wt% ZrO_2 [15]. Similarly, the mixed powders with a ratio of 66.5 wt% Al_2O_3 to 33.5 wt% Y_2O_3 were used for fabricating Al_2O_3/YAG parts [16]. The micrographs of the three powders are shown in Figure 2.

During the deposition experiment, the coupled nozzle and laser assembly moved back and forth in the *x*-*y* plane to perform ceramic deposition. After each layer deposition, the substrate together with the already deposited part was moved away from the nozzle by one layer thickness along the *z* direction so as to maintain a constant focus position for depositing the next layer. The process was then repeated to finish the single-bead wall. For different materials, the process parameters were different. Based on the systematic experiment, the optimum process parameters were obtained for the three powder materials, as shown in Table 1.

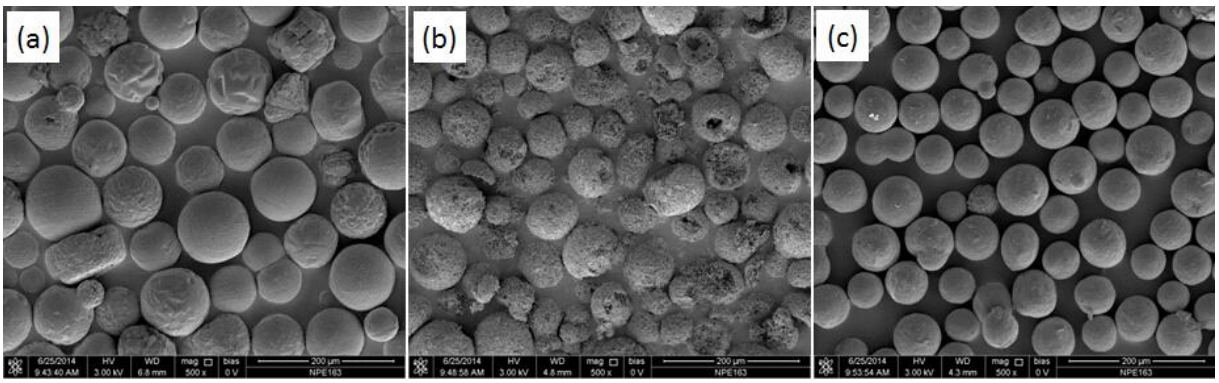

Figure 2 Ceramic powders used in the experiment (a) Al_2O_3; (b) Y_2O_3; (c) ZrO_2

Table 1 Process Parameters for the Ceramic Powders

Materials	Laser Power (W)	Nozzle Travel Speed (mm/min)	Powder Flow Rate (g/min)	Z-increment (mm)
Al_2O_3	350	300	1.36	0.22
Al_2O_3/Y_2O_3	320	350	1.08/0.55	0.18
Al_2O_3/ZrO_2	410	400	1.22/0.87	0.25

The fabricated ceramic parts were cut from the longitudinal cross-section A-A, as shown in Figure 3, and then prepared by coating a thin Au to observe the microstructure in a Scanning Electron Microscope (SEM). For the Al_2O_3/ZrO_2 and Al_2O_3/YAG ceramic parts, their cross-sections were polished with a diamond disk and an abrasive paper before being coated with Au. Vickers micro hardness measurements were made on the polished samples using a 1000 g load for 15 seconds, and an average value of 10 measurements on each sample was reported.

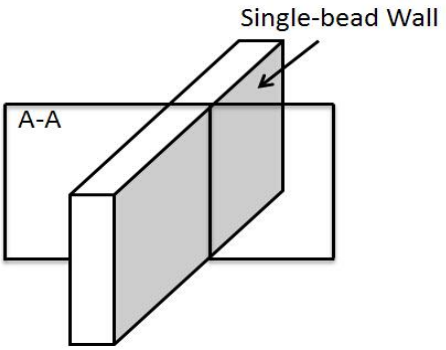

Figure 3 The longitudinal cross-section of a fabricated part

3. Results and discussion

3.1 Properties of deposited Al_2O_3 part

Figure 4(a) is a photographic view of a 50-layer Al_2O_3 single-bead wall fabricated from the Al_2O_3 powders under the process parameters shown in Table 1. Many stripes could be observed on the surface of the part, and cracks were found along the deposition direction, most of which in the middle portion of the part. On the other hand, a few cracks were found near the two side edges of the single-bead wall, but much longer than those in the middle portion. It should be noted that very few cracks were generated along the scanning direction.

Crack generation in Figure 4(a) may mainly be related to two factors: thermal stress during the laser depositing process and crystallographic orientation of the fabricated part [17]. Because laser scanning is a layer-by-layer process, highly non-uniform temperature distribution is formed across the deposited part. During the solidification process, volume contraction in the laser

scanning direction is constrained by the previously deposited layer with the first layer being constrained by the substrate. Consequently, thermal tensile stress occurs in the part along the laser scanning direction. Substrate temperature is usually lower than that of the ceramic part due to the good thermal conductivity of the substrate, resulting in the tensile stress in the first layer, which in turn generates a bending moment, as shown in Fig. 5. The thermal stress distribution of the fabricated ceramic part is similar to that of the metal parts, which has been reported in the literature [18-19]. On the other hand, it can be seen from Figure 4(b) that the microstructure of the fabricated part was comprised of directional columnar crystals along the deposition direction with an intergranular space of about 10-15 μm due to the directional heat dissipation [20]. It is easy for cracks to propagate along the crystal boundaries in the deposition direction, whereas it may be much harder to propagate along the scanning direction because more energy is needed for crack propagation through a crystal. Consequently, it is more preferable for a crack to form and propagate in the vertical direction than in the other directions. For the above reasons, vertical cracks are preferably generated (Figure 4(a)).

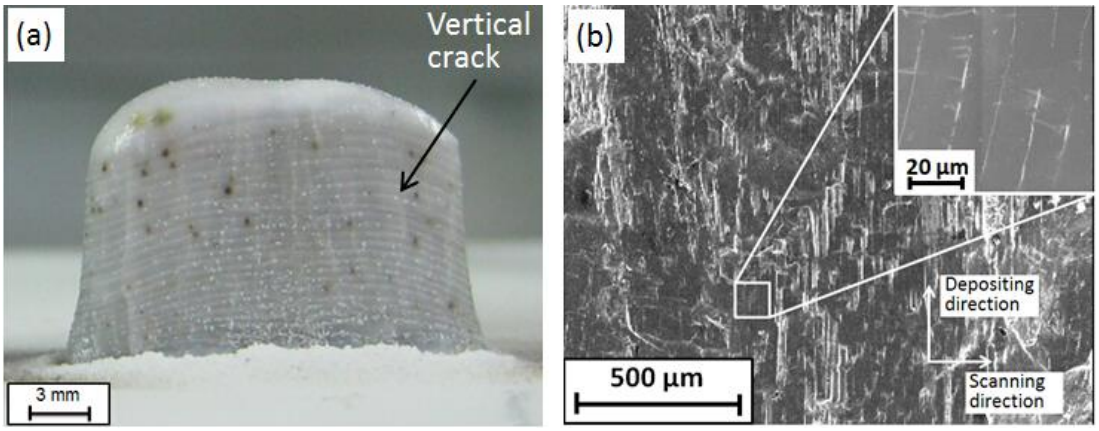

Figure 4 (a) Vertical cracks and (b) Microstructure of the deposited Al_2O_3 part

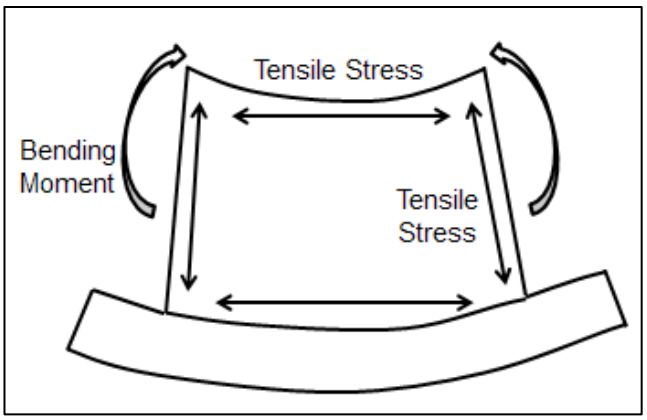

Figure 5 Bending moment and tensile stress induced by solidification contraction

The average micro-hardness of the deposited Al_2O_3 part was measured 1800 Hv, compared to 1600 Hv for the traditional Al_2O_3 ceramic materials. The hardness essentially rests with the

corundum structure of α-Al_2O_3 and its ionic (63%) and covalent (37%) bonding energies [21], whereas the LENS method results in the dense structure of a deposited part, which is because of its unique melting-solidification process.

3.2 Properties of deposited Al_2O_3 /YAG part

Figure 6(a) presents a photograph of a 50-layer Al_2O_3/YAG single-bead wall fabricated from the mixed ceramic powders at the eutectic ratio. During the fabrication process, the following chemical reactions could be used to describe the formation of $Y_3Al_5O_{12}$ (YAG) [22]. Then the rest of Al_2O_3 and the generated YAG should solidify simultaneously at 1826 ℃ to form the eutectic ceramics of Al_2O_3/YAG [22].

$$Al_2O_3 + 2Y_2O_3 \rightarrow Y_4Al_2O_9(\mathrm{YAM})\ (900-1100\ ℃) \quad (1)$$

$$Y_4Al_2O_9 + Al_2O_3 \rightarrow 4YAlO_3(\mathrm{YAP})\ (1100-1250\ ℃) \quad (2)$$

$$3YAlO_3 + Al_2O_3 \rightarrow Y_3Al_5O_{12}(\mathrm{YAG})\ (1400-1600\ ℃) \quad (3)$$

Compared with the Al_2O_3 part discussed above, a two phase ceramic part was deposited with fewer cracks. There were three vertical cracks in the depositing direction and two horizontal cracks in the scanning direction, which might be induced by a tensile stress in the corresponding directions. Shown in Figure 6(b), light-grey YAG phase evenly embeded in the Al_2O_3/YAG eutectic matrix. The volume fraction of the two phases did not seem to match the material ratio at the eutectic point, which might be due to the local evaporation of Al_2O_3 or the rapid solodification during the deposition process. The microstructure of the Al_2O_3/YAG single-bead wall was finer without obvious directional growth characteristics, which could help surpress both vertical and horizontal cracks. From the magnified image of Figure 6(b), a fine-grained microstructure with a eutectic spacing smaller than 1 μm is observed, resulting in the extremely complex interphase boundaries. Therefore, it would be difficult for a crack to initiate and propagate in such a fine-grained microstructure.

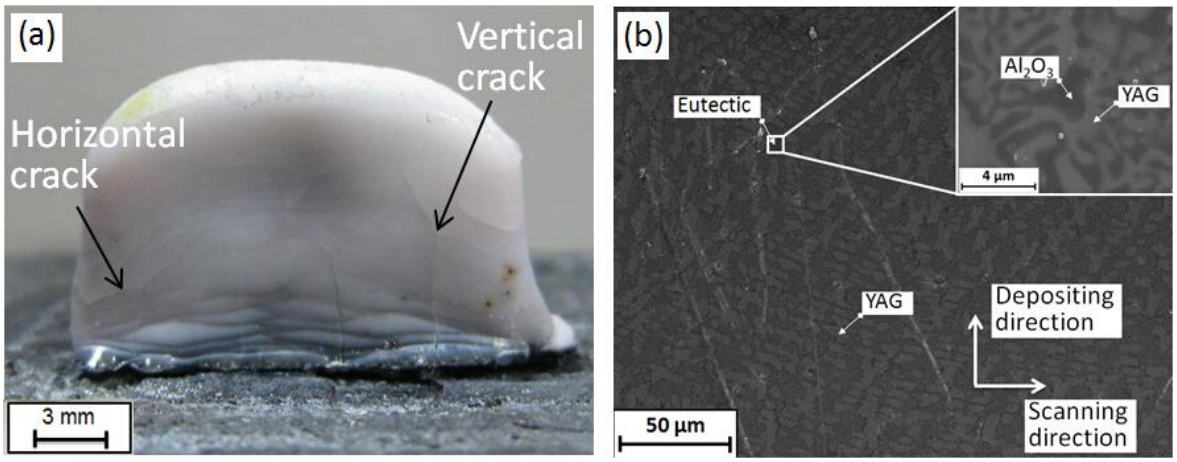

Figure 6 (a) Vertical and horizontal cracks and (b) Microstructure of Al_2O_3/YAG part

Based on the experimental measurement, the average micro-hardness of Al_2O_3/YAG was 1575 Hv, slightly lower than that of the Al_2O_3 ceramic part. The value was comparable to that of the traditional Al_2O_3/YAG eutectic ceramics made by the directional solidification or the laser-heated floating zone method [23,24].

3.3 Properties of deposited Al_2O_3 /ZrO_2 part

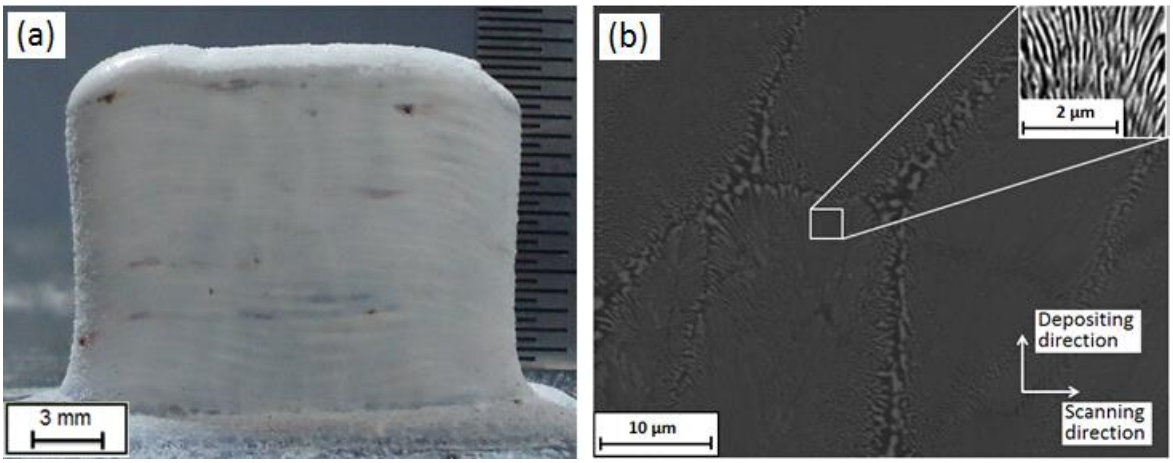

Figure 7 (a) Fabricated Al_2O_3/ZrO_2 part without cracks; (b) Microstructure of the Al_2O_3/ZrO_2 part

Figure 7(a) provides a photograph of a 60-layer Al_2O_3/ZrO_2 single-bead wall. The eutectic Al_2O_3/ZrO_2 part was successfully deposited with no cracks along both the depositing and the scanning directions. Compared with the deposited Al_2O_3/YAG ceramic part, the microstructure of Al_2O_3/ZrO_2 was also consisted of two phases, the black Al_2O_3 phase and the white ZrO_2 phase, but the eutectic spacing of Al_2O_3/ZrO_2 was nano-sized which was obviously finer than that of the eutectic Al_2O_3/YAG part in Figure 7(b). As a result, the eutectic Al_2O_3/ZrO_2 part can be made without cracks.

The micro-hardness of the traditional ZrO_2 is approximately 1200 Hv. However, the average hardness of the deposited eutectic Al_2O_3/ZrO_2 part reached 1715 Hv, although lower than that of the pure Al_2O_3, but higher than that of the Al_2O_3/ZrO_2 parts (an average value of 1460 Hv) made by the traditional methods.

3.4 Parts deposited for demonstration purpose

As mentioned above, the second-phase doping has been proven to be an effective method for suppressing cracks and refining microstructures during the direct fabrication process of ceramics by LENS. For the demonstration purpose, more eutectic Al_2O_3/ZrO_2 parts were deposited by this method. As shown in Figure 8, a cylindrical structure longer than 50 mm, an arc wall and a short cylinder were successfully fabricated with no cracks but good surface quality.

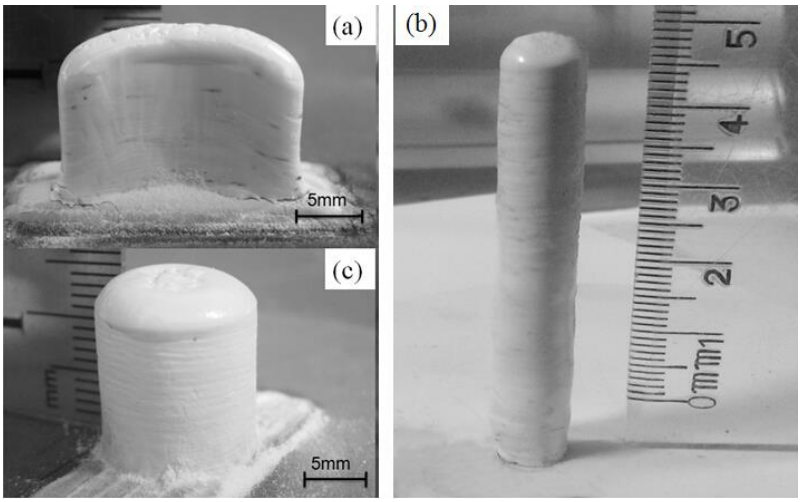

Figure 8 Al_2O_3/ZrO_2 parts of (a) Arc wall; (b) Long cylinder; (c) Short cylinder

4. Summary

Direct fabrication of Al_2O_3 ceramic single-bead walls is conducted by the LENS system in this study. Y_2O_3 and ZrO_2 are doped into Al_2O_3 powders respectively as a second-phase to restrict crack formation and improve microstructure of the deposited ceramic parts. The results show that both the second-phase doping of Y_2O_3 and ZrO_2 perform well in refining the microstructures of the direct laser deposited Al_2O_3/YAG and Al_2O_3/ZrO_2 ceramic parts, which suppresses crack formation. The micro-hardness investigation reveals that the second-phase doping does not result in much hardness reduction in Al_2O_3 and the two eutectic ceramics are both harder than 1500 Hv. The study indicates that second-phase doping is an effective way to improving laser deposition quality of ceramic parts.

Acknowledgements

The authors would like to acknowledge the financial support from the National Natural Science Foundation of China (No.51175061), the Science Fund for Creative Research Groups (No.51321004) and the China Postdoctoral Science Foundation Funded Project (No.2014M551072).

References

[1] D. Richerson, "Modern Ceramic Engineering: Properties, Processing, and Use in Design," CRC press, 2005.

[2] W. D. Kingery,, H. K. Bowen, D. R. Uhlmann, Introduction to Ceramics, 2nd Ed., 1976

[3] M. N. Rahaman. Ceramic Processing. John Wiley & Sons, Inc., 2006.

[4] H. C. Yen, "A New Slurry-based Shaping Process for Fabricating Ceramic Green Part by Selective Laser Scanning the Gelled Layer," Journal of the European Ceramic Society, 2012, 32(12), pp. 3123-3128.

[5] A. Licciulli, C. Esposito Corcione, A. Greco, V. Amicarelli and A. Maffezzoli, "Laser Stereolithography of ZrO_2 Toughened Al_2O_3," Journal of the European Ceramic Society, 2005, 25(9), pp. 1581-1589.

[6] J. Park, M. J. Tari, H. T. Hahn, "Characterization of the Laminated Object Manufacturing (LOM) Process," Rapid Prototyping Journal, 2000, 6(1), pp. 36-50.

[7] M. Allahverdi, S. C. Danforth, M. Jafari and A. Safari, "Processing of Advanced Electroceramic Components by Fused Deposition Technique," Journal of the European Ceramic Society, 2001, 21(10), pp. 1485-1490.

[8] T. Huang, M. S. Mason, X. Zhao, G. E. Hilmas and M. C. Leu, "Aqueous-based Freeze-form Extrusion Fabrication of Alumina Components," Rapid Prototyping Journal, 2009, 15(2), pp. 88-95.

[9] V. K. Balla, S. Bose, A. Bandyopadhyay, "Processing of Bulk Alumina Ceramics Using Laser Engineered Net Shaping," International Journal of Applied Ceramic Technology, 2008, 5(3), pp. 234-242.

[10] S. A. Bernard, V. K. Balla, S. Bose and A. Bandyopadhyay, "Direct Laser Processing of Bulk Lead Zirconate Titanate Ceramics," Materials Science and Engineering: B, 2010, 172(1), pp. 85-88.

[11] H. Yves-Christian, W. Jan, M. Wilhelm, W. Konrad and P. Reinhart, "Net Shaped High Performance Oxide Ceramic Parts by Selective Laser Melting," Physics Procedia, 2010, 5, pp. 587-594.

[12] W. Jan, H. Yves-Christian, M. Wilhelm, "Additive Manufacturing of ZrO_2-Al_2O_3 Ceramic Components by Selective Laser Melting," Rapid Prototyping Journal, 2013, 19(1), pp. 51-57.

[13] P, Bertrand, F, Bayle, C, Combe, P. Goeuriot and I. Smurov, "Ceramic Components Manufacturing by Selective Laser Sintering," Applied Surface Science, 2007, 254(4), pp. 989-992.

[14] I. Shishkovsky, I. Yadroitsev, P. Bertrand and I. Smurov, "Alumina–zirconium Ceramics Synthesis by Selective Laser Sintering/Melting," Applied Surface Science, 2007, 254(4), pp. 966-970.

[15] A. Larrea, G. F. De la Fuente, R. I. Merino and V. M. Orera, "ZrO_2–Al_2O_3 Eutectic Plates Produced by Laser Zone Melting," Journal of the European Ceramic Society, 2002, 22(2), pp. 191-198.

[16] Y. Waku, N. Nakagawa, T. Wakamoto, H. Ohtsubo, K. Shimizu and Y. Kohtotu, "A Ductile Ceramic Eutectic Composite with High Strength at 1,873 K," Nature, 1997, 389(6646), pp. 49-52.
[17] T. L. Anderson, Fracture Mechanics: Fundamentals and Applications, CRC press, 2005.
[18] M. L. Griffith, M. E. Schlienger, L. D. Harwell, M. S. Oliver, M. D. Baldwin, M. T. Ensz, M. Essien, J. Brooks, C. V. Robino, J. E. Smugeresky, W. H. Hofmeister, M. J. Wert, D. V. Nelson, "Understanding Thermal Behavior in the LENS Process," Materials and Design, 1999, 20, pp. 107-113.
[19] L. Wang, S. D. Felicelli, P. Pratt, "Residual Stresses in LENS-deposited AISI 410 Stainless Steel Plates," Material Science and Engineering A, 2008, 496, pp. 234-241.
[20] M. Gäumann, S. Henry, F. Cleton, J. D. Wagniere and W. Kurz, "Epitaxial Laser Metal Forming: Analysis of Microstructure Formation," Materials Science and Engineering: A, 1999, 271(1), pp. 232-241.
[21] W. Chen, "Study on the Microstructure Evolution of α-Al_2O_3 in the Formation Process and It's Controlling," Central South University, 2010.
[22] O. Fabrichnaya, H. J. Seifert, T. Ludwig, F. Aldinger and A. Navrotsky, "The Assessment of Thermodynamic Parameters in the Al_2O_3–Y_2O_3 System and Phase Relations in the Y–Al–O System," Scandinavian Journal of Metallurgy, 2001, 30(3), pp. 175-183.
[23] A. Larrea, V. M. Orera, R. I. Merino and J. I. Pena, "Microstructure and Mechanical Properties of Al_2O_3–YSZ and Al_2O_3–YAG Directionally Solidified Eutectic Plates," Journal of the European Ceramic Society, 2005, 25(8), pp. 1419-1429.
[24] J. Y. Pastor, J. LLorca, A. Salazar, P. B. Oliete, I. D. Francisco and J. I. Pena, "Mechanical Properties of Melt Grown Alumina–Yttrium Aluminum Garnet Eutectics up to 1900 K," Journal of the American Ceramic Society, 2005, 88(6), pp. 1488-1495.